FTC of Three-phase Induction Motor Drives under Current Sensor Faults

Azizollah Gholipour[1], Mahmood Ghanbari[1*], Esmaeil Alibeiki[2], Mohammad Jannati[1]

Abstract – In this study, single-phase current sensor Fault-Tolerant Control (FTC) for Three-Phase Induction Motor (TPIM) drives using a flux observer is proposed. In the proposed FTC scheme, a 3rd difference operator executes the Fault Detection (FD) task and the reconstruction of the faulted current is achieved through a flux observer. The presented FTC system is able to switch TPIM drive systems from normal mode to the faulty mode suitably. The proposed method in this study can be utilized in many industries particularly in electric vehicles, medical devices, and aerospace where TPIM drive systems are needed to continue the desired operation even during fault situations. The effectiveness of the proposed FTC system is confirmed by experiments on a 0.75kW TPIM drive platform.

Nomenclature

$[v_{dq0s}^s]$, $[v_{dq0r}^s]$	Stator and rotor voltage matrices
$[i_{dq0s}^s]$, $[i_{dq0r}^s]$	Stator and rotor current matrices
$[\varphi_{dq0s}^s]$, $[\varphi_{dq0r}^s]$	Stator and rotor flux matrices
p	Differential operator
r_s, r_r	Stator and rotor resistances
l_s, l_r, l_m	Stator and rotor self and magnetizing inductances
l_{ls}, l_{lr}	Stator and rotor leakage inductances
Ω_e, Ω_r	Rotating and rotor speeds
T_e	Electromagnetic torque
i_{qs}^e, i_{dr}^e, i_{ds}^e, i_{qr}^e	Stator and rotor dq currents
$|\varphi_r|$, β_e	Rotor flux angle and amplitude
i_{as}, i_{bs}	Motor currents
k	Predefined threshold
φ_{ds}^e, φ_{qs}^e, φ_{dr}^e, φ_{qr}^e	Stator and rotor dq fluxes
φ_{dm}^e, φ_{qm}^e	Mutual fluxes
v_{ds}^e, v_{qs}^e	Stator dq voltages
Superscripts "s", "e"	Stationary and rotating reference frames
Superscripts "^", "*"	Estimated and reference values

1*   Corresponding Author : Department of Electrical Engineering, Gorgan Branch, Islamic Azad University, Gorgan, Iran. Email: ghanbari@gorganiau.ac.ir

2 Department of Electrical Engineering, Aliabad Katoul Branch, Islamic

Azad University, Aliabad Katoul, Iran

1. Introduction

Three-Phase Induction Motor (TPIM) drives have been widely utilized in many industries due to their simple construction, low price, and high efficiency [1-3]. Field-Oriented Control (FOC) strategies can be considered as powerful control techniques for TPIM drives [4-6]. Despite the good performance of FOC strategies during normal conditions, they are not suitable for abnormal situations such as fault conditions.

In general, faults on the drive systems can be classified as faults on the converter [7], faults on the machine [8], and faults on the sensors [9]. The converter faults are normally related to power switch open-circuit faults and power switch short-circuit faults. Faults on the machine include open-circuit/short-circuit faults of the stator windings, rotor faults, and faults on the mechanical parts. Finally, sensor faults include electrical or mechanical faults which can be happened on the speed sensor, current sensor, etc.

Based on this classification, different Fault-Tolerant Control (FTC) methods have been proposed to control TPIM drives. In general, FTC methods are divided into two categories [10]: passive FTC systems and active FTC systems. In passive control systems, a robust control method such as H∞ is utilized for healthy and faulty drive systems. Despite simple structure of these systems, they are not optimized during both healthy and faulty conditions. In active control systems, a conventional control system is used for pre-fault operation. After Fault Detection (FD), a new control method is applied for the post-fault operation. These control methods have good performances during both healthy and faulty conditions.

Current sensors are needed in FOC strategies of TPIM drives. Nevertheless, current sensors are subject to different

electrical/mechanical faults which reduce the security and dependability of TPIM drive systems. Single-phase current sensor fault is one of the most common faults in TPIM drive systems. Failure of current sensors reduces the performance of TPIM drive systems even leads to the breakdown of FOC strategies.

Different strategies have been suggested for detection of current sensor faults as well as TPIM control in this condition. In [11], a method for FTC of a TPIM drive based on Direct Torque Control (DTC) method under current sensor faults was presented. In [11], a leakage flux observer was used to estimate the motor currents in the faulty mode. In [12], a FTC system based on adaptive fuzzy observer and using the DTC method was proposed to drive a TPIM during speed and current sensor faults. In [12], a residual signal was used to detect the fault, which causes a time delay. In [13, 14] different methods were proposed for the sensor FD using neural networks with the assistance of motor currents and voltages, motor speed, measured torque, rated power, and DC link voltage values. These methods are very difficult to implement for practical applications. In [15], an observer with a residual signal was proposed for FTC of TPIM drives against current sensor and DC link voltage sensor faults. In the proposed scheme in [15], open-loop estimators were used for each sensor. Therefore, this design is not suitable for applications that require a precise speed control. In [16], an advanced Kalman filter with an adaptive flux observer to detect current sensor faults was presented. This method also has high computational complexity and it is time consuming. In [17], three different control schemes were used for FTC of a TPIM drive. In this paper, when a speed sensor fault occurs, the control system switches to the speed sensorless control. During the current sensor fault, the control system switches to the closed-loop scalar control method if the speed sensor is healthy and the open-loop scalar control method if the speed sensor is not healthy. The proposed control system in [17] increases the complexity of the drive system and it is not suitable for industrial applications.

In this research, an active FTC method for TPIM drives against single-phase current sensor fault is proposed. In the proposed FTC strategy, a 3rd difference operator is used for the FD. In addition, the reconstruction of the faulted current is achieved through a flux observer. The main goal of this research is to achieve a desired performance for the faulty drive system similar to a healthy drive system after single-phase current sensor fault. Compared to [11], the proposed method in this paper does not require the voltage sensor and it has high accuracy due to using FOC method instead of DTC method. The usefulness of the proposed strategy is checked by experiments using DSP/TMS320F28335 controller board.

2. Modelling and FOC of a TPIM

The TPIM model can be expressed by (1)-(5) [18]:

$$[v_{dq0s}^s] = \begin{bmatrix} r_s + l_s p & 0 & 0 \\ 0 & r_s + l_s p & 0 \\ 0 & 0 & r_s + l_{ls} p \end{bmatrix} [i_{dq0s}^s] +$$
$$\begin{bmatrix} l_m p & 0 & 0 \\ 0 & l_m p & 0 \\ 0 & 0 & 0 \end{bmatrix} [i_{dq0r}^s]$$

$$(1)$$

$$[v_{dq0r}^s] =$$
$$\begin{bmatrix} l_m p & \Omega_r l_m & 0 \\ -\Omega_r l_m & l_m p & 0 \\ 0 & 0 & 0 \end{bmatrix} [i_{dq0s}^s] +$$
$$\begin{bmatrix} r_r + l_r p & \Omega_r l_r & 0 \\ -\Omega_r l_r & r_r + l_r p & 0 \\ 0 & 0 & r_r + l_{lr} p \end{bmatrix} [i_{dq0r}^s]$$

$$(2)$$

$$[\varphi_{dq0s}^s] =$$
$$\begin{bmatrix} l_{ls} + l_m & 0 & 0 \\ 0 & l_{ls} + l_m & 0 \\ 0 & 0 & l_{ls} \end{bmatrix} [i_{dq0s}^s] + \begin{bmatrix} l_m & 0 & 0 \\ 0 & l_m & 0 \\ 0 & 0 & 0 \end{bmatrix} [i_{dq0r}^s]$$

$$(3)$$

$$[\varphi_{dq0r}^s] =$$
$$\begin{bmatrix} l_m & 0 & 0 \\ 0 & l_m & 0 \\ 0 & 0 & 0 \end{bmatrix} [i_{dq0s}^s] + \begin{bmatrix} l_{lr} + l_m & 0 & 0 \\ 0 & l_{lr} + l_m & 0 \\ 0 & 0 & l_{lr} \end{bmatrix} [i_{dq0r}^s]$$

$$(4)$$

$$T_e = \left(\frac{pole}{2}\right) l_m (i_{qs}^s i_{dr}^s - i_{ds}^s i_{qr}^s)$$

$$(5)$$

The FOC strategy is based on the orientation of the flux and it is generally classified as rotor FOC methods and stator FOC methods. In rotor FOC methods, the rotor flux is aligned with d-axis. Based on this assumption, the stator d-axis current indicates the rotor flux and the stator q-axis current indicates the electromagnetic torque. It means that the TPIM control can be simplified to an easy control system like separately excited DC motor [19]. Based on (1)-(5), the structure of the standard rotor FOC method can be shown as Figure 1 [18]:
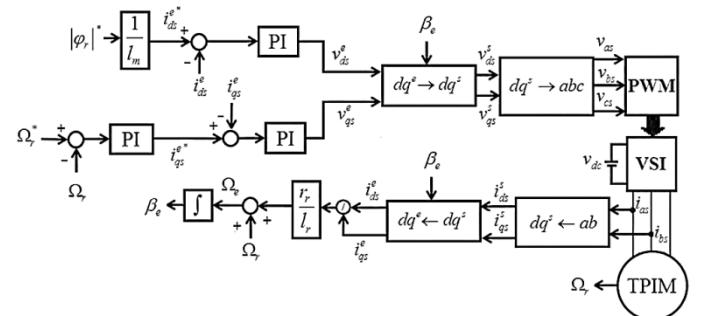
Figure 1. Structure of the standard rotor FOC method

3. Structure of the proposed FTC method

The structure of the proposed FTC method for a TPIM drive system is shown in Figure 2.
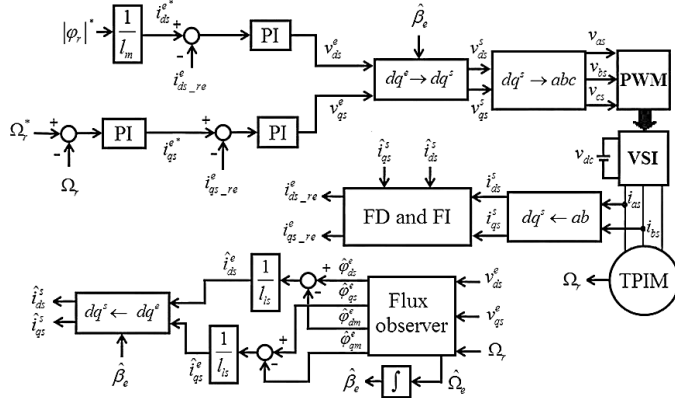
Figure 2. Structure of the proposed FTC method

In Figure 2 [18]:

$$\begin{bmatrix} i^e_{ds\_re} \\ i^e_{qs\_re} \end{bmatrix} = \begin{bmatrix} \cos\hat{\beta}_e & \sin\hat{\beta}_e \\ -\sin\hat{\beta}_e & \cos\hat{\beta}_e \end{bmatrix} \begin{bmatrix} i^s_{ds\_re} \\ i^s_{qs\_re} \end{bmatrix}$$

(6)

The proposed FTC system in Figure 2 includes a rotor FOC strategy, FD and Fault Isolation (FI) mechanisms, and a flux observer.

According to Figure 2, the estimated values of the TPIM currents are obtained using the flux observer and some simple calculations. In the proposed scheme, after detection and isolation of the fault, the proper values of the currents are selected to continue the uninterrupted operation of the TPIM drive system. In Figure 2 and under normal condition, the actual motor currents are used for the FOC system. Under this condition, the drive system has similar structure with the standard rotor FOC strategy. In other words, the only difference between the proposed method and the standard rotor FOC during normal mode is that in the proposed strategy the rotor flux angle is achieved using the integration of $\hat{\Omega}_e$ and in the standard FOC technique the rotor flux angle is achieved based on the motor currents, speed, and a pure integration. In Figure 2, when the fault occurs, the corresponding estimated values of currents are used for the FOC system.

4. FD mechanism

As can be observed from Figure 2, two current sensors are used to measure the currents. In this paper, two 3rd difference operators (Δ^3) are utilized to the current sensor FD. The 3rd difference operator for phases "a" and "b" can be expressed by (7)-(12) [20]:

$$\Delta^3 i_{as/bs} = \Delta^2 i_{as1/bs1} - \Delta^2 i_{as0/bs0}$$

(7)

where,

$$\Delta^2 i_{as0/bs0} = \Delta i_{as1/bs1} - \Delta i_{as0/bs0}$$

(8)

$$\Delta^2 i_{as1/bs1} = \Delta i_{as2/bs2} - \Delta i_{as1/bs1}$$

(9)

$$\Delta i_{as0/bs0} = i_{as1/bs1} - i_{as0/bs0}$$

(10)

$$\Delta i_{as1/bs1} = i_{as2/bs2} - i_{as1/bs1}$$

(11)

$$\Delta i_{as2/bs2} = i_{as3/bs3} - i_{as2/bs2}$$

(12)

The current sensor FD is based on the comparison between the absolute values of the 3rd difference operators with a predefined threshold (k) as [11, 20]:
- ➤ if $|\Delta^3 i_{as}| \geq k \& |\Delta^3 i_{bs}| \geq k$, both sensors fail
- ➤ if $|\Delta^3 i_{as}| \geq k \& |\Delta^3 i_{bs}| < k$, "a" phase sensor fails and "b" phase sensor is healthy
- ➤ if $|\Delta^3 i_{as}| < k \& |\Delta^3 i_{bs}| \geq k$, "a" phase sensor is healthy and "b" phase sensor fails
- ➤ if $|\Delta^3 i_{as}| < k \& |\Delta^3 i_{bs}| < k$, both sensors are healthy

5. FI mechanism

According to Figure 2, the motor currents are transformed from ab frame to dqs frame using (13) [18]:

$$\begin{bmatrix} i^s_{ds} \\ i^s_{qs} \end{bmatrix} = \begin{bmatrix} 1 & 0 \\ \frac{\sqrt{3}}{3} & \frac{2\sqrt{3}}{3} \end{bmatrix} \begin{bmatrix} i_{as} \\ i_{bs} \end{bmatrix}$$

(13)

As can be seen from (13), the current of d-axis is independent from the current of b-axis. In addition, the current of q-axis depends on a-axis and b-axis currents. In other words, the estimated values of currents should be used when the current sensor fault occurs in phase "a". Furthermore, when a current sensor fault occurs in phase "b", the estimated value of stator q-axis current and the actual value of stator d-axis current should be used. When the fault does not occur and the motor is in normal condition, the actual values of motor dq currents should be utilized.

6. Reconstruction of the motor currents using a flux observer

In this section, the estimation technique for motor currents is presented. In the rotating reference frame, the

mutual and stator fluxes can be obtained as (14) and (15), respectively [11]:

$$\begin{bmatrix} \widehat{\varphi}_{dm}^e \\ \widehat{\varphi}_{qm}^e \end{bmatrix} = \begin{bmatrix} \frac{l_{m1}}{l_{ls}} & 0 & \frac{l_{m1}}{l_{lr}} & 0 \\ 0 & \frac{l_{m1}}{l_{ls}} & 0 & \frac{l_{m1}}{l_{lr}} \end{bmatrix} \begin{bmatrix} \widehat{\varphi}_{ds}^e \\ \widehat{\varphi}_{qs}^e \\ \varphi_{dr}^e \\ \varphi_{qr}^e \end{bmatrix}$$

(14)

$$\begin{bmatrix} p\widehat{\varphi}_{ds}^e \\ p\widehat{\varphi}_{qs}^e \end{bmatrix} = \begin{bmatrix} -\frac{r_s}{l_{ls}} & \widehat{\Omega}_e & \frac{r_s}{l_{ls}} & 0 \\ -\widehat{\Omega}_e & -\frac{r_s}{l_{ls}} & 0 & \frac{r_s}{l_{ls}} \end{bmatrix} \begin{bmatrix} \widehat{\varphi}_{ds}^e \\ \widehat{\varphi}_{qs}^e \\ \varphi_{dm}^e \\ \varphi_{qm}^e \end{bmatrix} + \begin{bmatrix} v_{ds}^e \\ v_{qs}^e \end{bmatrix}$$

(15)

where, [11]

$$l_{m1} = \frac{l_m l_{ls} l_{lr}}{l_{ls} l_{lr} + l_m l_{lr} + l_m l_{ls}}$$

(16)

$$\widehat{\Omega}_e = \Omega_r + \frac{\widehat{\varphi}_{ds}^e \widehat{i}_{qs}^e - \widehat{\varphi}_{qs}^e \widehat{i}_{ds}^e}{2\left(\widehat{\varphi}_{dm}^{e\ 2} + \widehat{\varphi}_{qm}^{e\ 2}\right)} r_r$$

(17)

According to the rotor FOC strategy, the values of rotor fluxes in (14) are obtained as [18]:

$$\varphi_{dr}^e = |\varphi_r|^*$$

(18)

$$\varphi_{qr}^e = 0$$

(19)

In the rotating reference frame, the stator currents in terms of fluxes can be written as [21]:

$$\begin{bmatrix} \widehat{i}_{ds}^e \\ \widehat{i}_{qs}^e \end{bmatrix} = \begin{bmatrix} \frac{1}{l_{ls}} & 0 & -\frac{1}{l_{ls}} & 0 \\ 0 & \frac{1}{l_{ls}} & 0 & -\frac{1}{l_{ls}} \end{bmatrix} \begin{bmatrix} \widehat{\varphi}_{ds}^e \\ \widehat{\varphi}_{qs}^e \\ \widehat{\varphi}_{dm}^e \\ \widehat{\varphi}_{qm}^e \end{bmatrix}$$

(20)

As a result, based on (14)-(20), the motor currents can be estimated (see Figure 2).

7. Experimental results

In this section, the performance of the proposed FTC strategy for a TPIM drive system controlled by the rotor FOC method is validated using the DSP/TMS320F28335 controller board. The picture of the test set-up for a 0.75kW TPIM is shown in Figure 3.
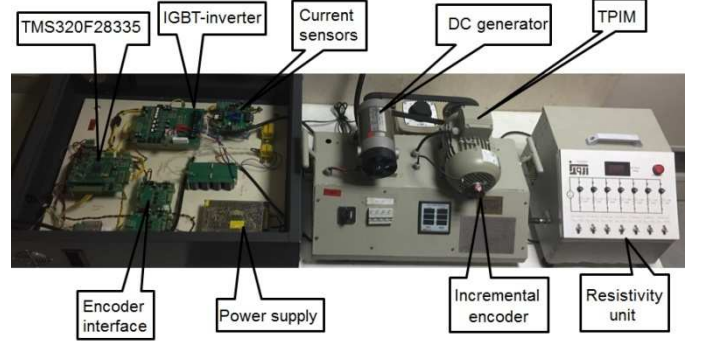
Figure 3. Test set-up

In tests, the rotor flux command is set to 1wb. The proposed FTC system code used in DSP is generated using PSIM software at the sampling frequency of 10kHz. The current sensor fault in this paper is emulated by making the sensed current to zero. The TPIM specifications are given in Table 1.

Table 1. TPIM specifications

r_s	r_r	l_s, l_r	l_{ls}, l_{lr}	$pole$	j
10.44Ω	14.64Ω	0.61H	0.014H	4	0.016kg.m2

7.1. Performance of the proposed FTC strategy when "a" phase sensor is healthy and "b" phase sensor fails

The results of the introduced FTC system when "a" phase sensor is healthy and "b" phase sensor fails are shown in Figure 4. In this figure, the reference speed changes from 30rad/s to 45rad/s at t=17.15s.

Figure 4 shows the good performance of the introduced FTC system in both normal and current sensor failure modes. The actual and estimated currents shown in this figure indicate that the actual d-axis current after the fault has a correct value. However, the actual q-axis current is affected by the fault and produces an incorrect value. As mentioned before, in this condition the actual d-axis current and the estimated q-axis current are used in the control system.

7.2. Performance of the proposed FTC strategy when "a" phase sensor fails and "b" phase sensor is healthy

The results of the introduced FTC system when "a" phase sensor fails and "b" phase sensor is healthy are shown in Figure 5. In this figure, the reference speed is 20rad/s.

As shown in Figure 5, the actual and reference speeds follow each other in both healthy and faulty conditions. Under such condition, both actual motor currents are affected and produce incorrect values. In this condition, the actual currents are replaced by the estimated currents. From

the experimental results of Figure 5 it can be seen that the TPIM drive system can be successfully changed from the rotor FOC method to the proposed FTC system.

estimate the motor currents. Experimental results confirm the good performance of the proposed FTC system during various conditions. Based on the results the performance of the proposed FTC system during normal and single-phase current sensor fault is nearly the same.
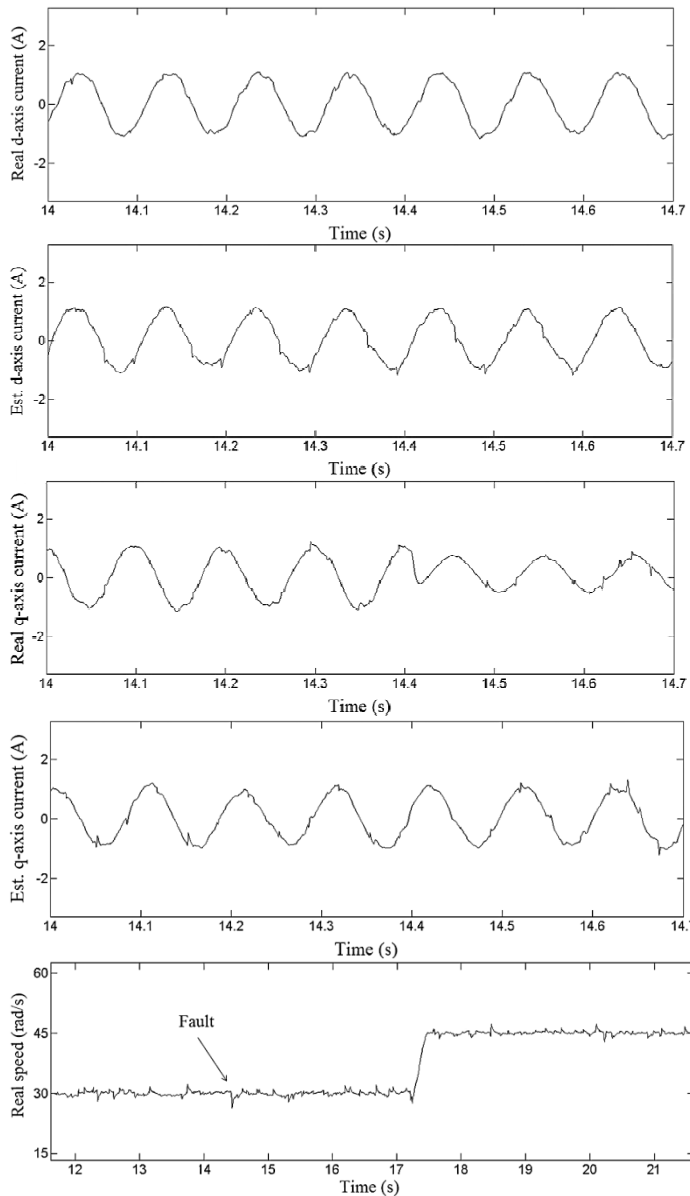
Figure 4. Experimental results of the proposed FTC strategy when "a" phase sensor is healthy and "b" phase sensor fails
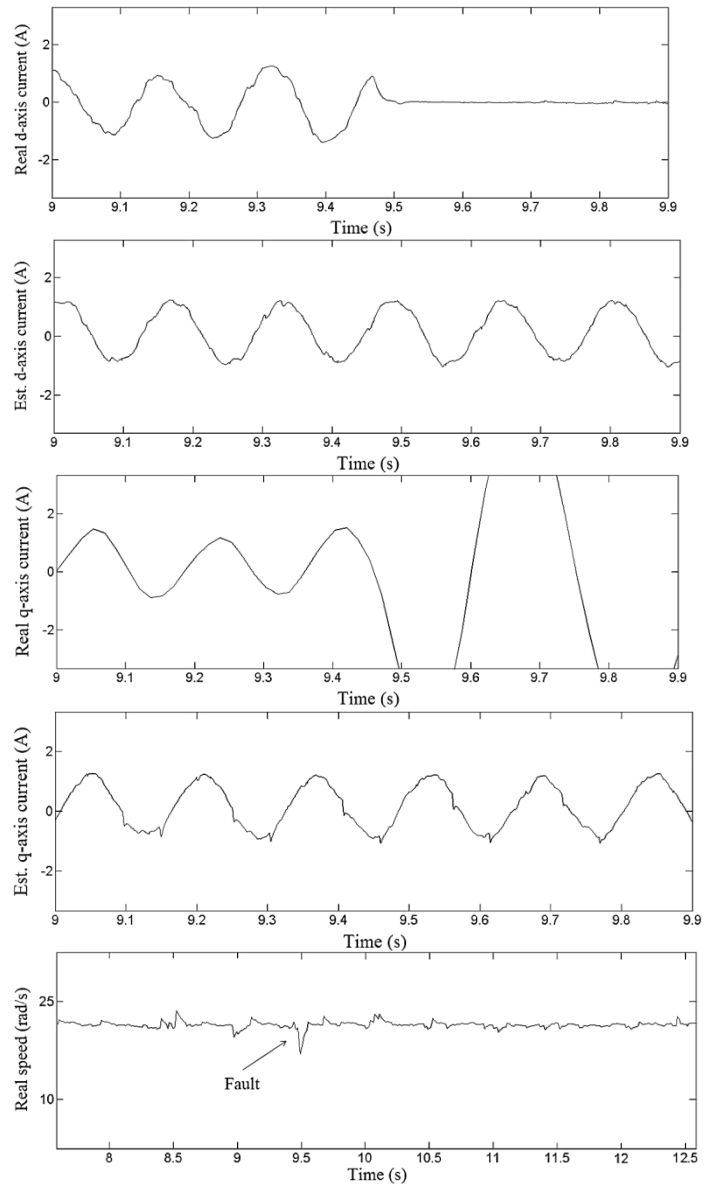
Figure 5. Experimental results of the proposed FTC strategy when "a" phase sensor fails and "b" phase sensor is healthy

8. Conclusion

This paper presents an active FTC scheme for TPIM drives against current sensor faults. In the proposed FTC scheme, a 3rd difference operator is used to detect the current sensor fault. In normal condition, the 3rd difference operator value is very small. However, in the faulty mode, the 3rd difference operator value related to the faulted current sensor has high value compared to the normal condition. After FD and FI, a flux observer is used to

References

[1] T. H. dos Santos, et al., "Scalar control of an induction motor using a neural sensorless technique," Electric power systems research, vol. 108, pp. 322-330, Mar 2014.

[2] S. A. R. Kashif, et al., "Implementing the induction-motor drive with four-switch inverter: An application of

neural networks," Expert Systems with Applications, vol. 38, pp. 11137-11148, Sep 2011.

[3] R. Tabasian, et al., "Direct field-oriented control strategy for fault-tolerant control of induction machine drives based on EKF," IET Electric Power Applications, Apr 2020.

[4] M. Jannati, et al., "Experimental evaluation of FOC of 3-phase IM under open-phase fault," International Journal of Electronics, vol. 104, pp. 1675-1688, Oct 2017.

[5] M. A. Hannan, et al., "Optimization techniques to enhance the performance of induction motor drives: A review," Renewable and Sustainable Energy Reviews, vol. 81, pp. 1611-1626, Jan 2017.

[6] S. Shukla and B. Singh, "Single-stage PV array fed speed sensorless vector control of induction motor drive for water pumping," IEEE transactions on industry applications, vol. 54, pp. 3575-3585, Feb 2018.

[7] B. S. G. Yelamarthi and S. R. Sandepudi, "Predictive Torque Control of Three-Phase Induction Motor Drive with Inverter Switch Fault-Tolerance Capabilities," IEEE Journal of Emerging and Selected Topics in Power Electronics, Aug 2020.

[8] M. Jannati, et al., "Vector control of star-connected 3-phase induction motor drives under open-phase fault based on rotor flux field-oriented control," Electric Power Components and Systems, vol. 44, pp. 2325-2337, Dec 2016.

[9] Y. Liu, et al., "Smooth fault-tolerant control of induction motor drives with sensor failures," IEEE Transactions on Power Electronics, vol. 34, pp. 3544-3552, Jun 2018.

[10] A. A. Amin and K. M. Hasan, "A review of fault tolerant control systems: advancements and applications," Measurement, vol. 143, pp. 58-68, Sep 2019.

[11] M. Manohar and S. Das, "Current sensor fault-tolerant control for direct torque control of induction motor drive using flux-linkage observer," IEEE Transactions on Industrial Informatics, vol. 13, pp. 2824-2833, Jun 2017.

[12] K. S. Lee and J. S. Ryu, "Instrument fault detection and compensation scheme for direct torque controlled induction motor drives," IEE Proceedings-Control Theory and Applications, vol. 150, pp. 376-382, Jul 2003.

[13 A. Bernieri, et al., "A neural network approach to instrument fault detection and isolation," In 10th Instrumentation and Measurement Technology Conference, pp. 139-144, May 1994.

[14] G. Betta, et al., "An advanced neural-network-based instrument fault detection and isolation scheme," IEEE transactions on instrumentation and measurement, vol. 47, pp. 507-512, Apr 1998.

[15] A. B. Youssef, et al., "State observer-based sensor fault detection and isolation, and fault tolerant control of a single-phase PWM rectifier for electric railway traction," IEEE transactions on Power Electronics, vol. 28, pp. 5842-5853,May 2013.

[16] X. Zhang, et al., "Sensor fault detection, isolation and system reconfiguration based on extended Kalman filter for induction motor drives," IET Electric Power Applications, vol. 7, pp. 607-617, Aug 2013.

[17] D. Diallo, et al., "A fault-tolerant control architecture for induction motor drives in automotive applications," IEEE transactions on vehicular technology, vol. 53, pp. 1847-1855, Nov 2004.

[18] P. Vas, "Sensorless vector and direct torque control," Oxford Univ. Press, 1998.

[19] M. Jannati, et al., "A review on Variable Speed Control techniques for efficient control of Single-Phase Induction Motors: Evolution, classification, comparison," Renewable and Sustainable Energy Reviews, vol. 75, pp. 1306-1319, Aug 2017.

[20] Y. C. Kang, et al., "A CT saturation detection algorithm," IEEE Transactions on Power Delivery, vol. 19, pp. 78-85, Jan 2004.

[21] B. K. Bose, "Modern power electronics and AC drives," Upper Saddle River, NJ, Prentice hall, 2002.